# Floating phase in the one-dimensional transverse axial next-nearest-neighbor Ising model

Anjan Kumar Chandra and Subinay Dasgupta

*Department of Physics, University of Calcutta, 92 Acharya Prafulla Chandra Road, Calcutta 700009, India*
(Received 26 September 2006; published 7 February 2007)

To study the ground state of an axial next-nearest-neighbor Ising chain under transverse field as a function of frustration parameter $\kappa$ and field strength $\Gamma$, we present here two different perturbative analyses. In one, we consider the (known) ground state at $\kappa = 0.5$ and $\Gamma = 0$ as the unperturbed state and treat an increase of the field from 0 to $\Gamma$ coupled with an increase of $\kappa$ from 0.5 to $0.5 + r\Gamma/J$ as perturbation. The first-order perturbation correction to eigenvalue can be calculated exactly and we could conclude that there are only two phase-transition lines emanating from the point $\kappa = 0.5$, $\Gamma = 0$. In the second perturbation scheme, we consider the number of domains of length 1 as the perturbation and obtain the zeroth-order eigenfunction for the perturbed ground state. From the longitudinal spin-spin correlation, we conclude that floating phase exists for small values of transverse field over the entire region intermediate between the ferromagnetic phase and antiphase.

PACS number(s): 64.60.Fr, 75.10.Jm, 05.50.+q

## I. INTRODUCTION

The transverse axial next-nearest neighbour Ising (ANNNI) model is one of the simplest Ising models that contains tunable frustration and tunable quantum fluctuation. In one dimension, it is defined (for spin=$\frac{1}{2}$) by the Hamiltonian [1]

$$\mathcal{H} = -J\sum_{h=1}^{N} (s_j^z s_{j+1}^z - \kappa s_j^z s_{j+2}^z) - \Gamma\sum_{j=1}^{N} s_j^x. \qquad (1)$$

Here the first term describes a ferromagnetic nearest-neighbor interaction of strength $J(>0)$ between longitudinal components of spin $s^z$ ($=\pm1$), the second term describes an antiferromagnetic second-neighbor interaction of strength $\kappa J$ also in the longitudinal direction, and the third term describes an external field in the transverse direction of strength $\Gamma$. The ratio $\kappa(>0)$ is called the frustration parameter. This Hamiltonian describes a classical ANNNI chain subjected to a transverse field as well as a transverse (nearest-neighbor) Ising model with an additional frustrated second-nearest-neighbor interaction. In this paper, we shall deal with the *ground-state* (zero-temperature) phase diagram of the Hamiltonian $\mathcal{H}$. It is known [1,2] that for $\kappa=0$ (only nearest-neighbor interaction), there is a ferromagnetic to paramagnetic second-order phase transition at $\Gamma=J$. On the other hand, for $\Gamma=0$ (classical ANNNI chain)[1,3] the ground state is ferromagnetic for $\kappa<0.5$ and antiphase ($++--$ type) for $\kappa>0.5$, with a "multiphase point" at $\kappa=0.5$. At the multiphase point [3] the ground state has very high [$\sim g^N$, where $g$ is the golden ratio $(\sqrt{5}+1)/2$] degeneracy as any combination of antiphase and ferromagnetic patches will serve as ground-state configuration. From approximate analytic and numerical approaches [1,4], early studies had proposed a phase diagram (Fig. 1) that consisted of ferromagnetic, paramagnetic, and antiphase regions, along with a region of what is called *floating phase*. The $n$th-neighbor spin-spin correlation function in the longitudinal direction

$$C^z(n) \equiv \langle s_j^z s_{j+n}^z \rangle - \langle s_j^z \rangle^2 \qquad (2)$$

decays exponentially with distance in the ferromagnetic, antiphase, and paramagnetic regions but decays algebraically in the floating phase. The evidence for the presence of a floating phase is provided by quantum Monte Carlo simulation [5] and by exact numerical diagonalization of small systems [4,6], one of which [4] extends even up to a length of 32.

Recently, a question has arisen on the existence of the floating phase, although a recent study [7] has claimed that the floating phase exists over a region as shown in Fig. 1. The transverse ANNNI chain is related to the two-dimensional classical ANNNI model by the Suzuki-Trotter transformation. The phase diagram for this model is also similar to Fig. 1 (with $\Gamma$ replaced by temperature). Here also the earlier studies [3] support the existence of a floating phase in view of Monte Carlo simulations by Selke and others [8] and approximate analytic calculations by Villain and Bak [9], while a recent measurement of dynamical exponent [10] and a density-matrix renormalization group analysis [11] claim that the floating phase exists, if at all, along a line only. We have also studied [12] some static and dynamical
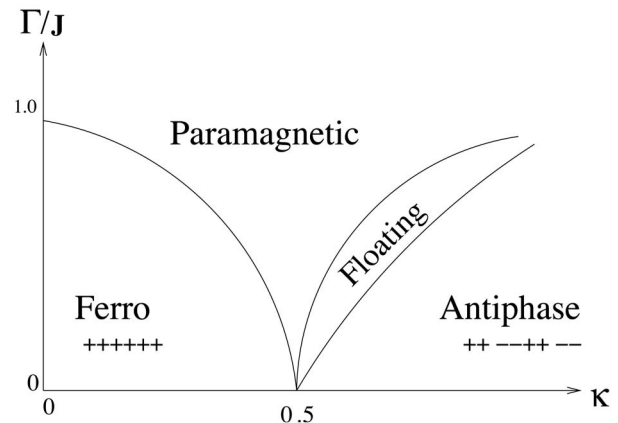


FIG. 1. Schematic phase diagram of the transverse ANNNI model according to early investigations [1,2].
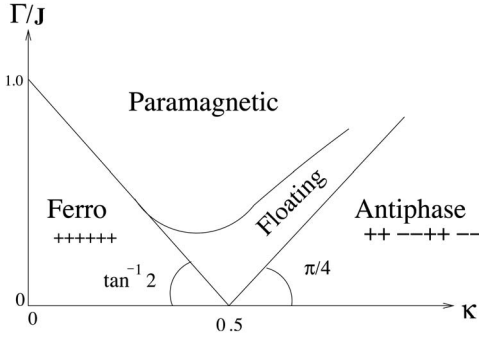
FIG. 2. Schematic phase diagram of the transverse ANNNI model according to the present work.
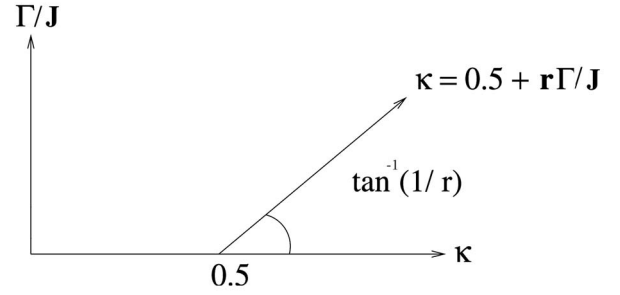


FIG. 3. Scheme of the first perturbation treatment. The transverse field is altered from zero to a (small) value $\Gamma$ and the frustration parameter $\kappa$ is altered from 0.5 to $0.5+r\Gamma/J$. The parameter $r$ may vary from $-\infty$ to $\infty$.

properties of the two-dimensional (2D) ANNNI model by Monte Carlo simulation. Our study also indicates that the floating phase exists, if at all, only along a line. The question as to whether the floating phase exists only along a line or extends over a region in the case of transverse ANNNI chain is the basic motivation of this paper.

In this paper we perform two perturbation calculations with an aim to have an idea about the phase that exists near the multiphase point for a nonzero transverse field. Our conclusion is that there exists a floating phase over a region extending from the ferromagnetic phase to the antiphase (for small values of $\Gamma$) and the phase diagram looks like Fig. 2. This result is in contradiction with previous results as none of the previous studies had predicted a floating phase for $\kappa < 0.5$. We must mention that all our results are true only at "small" values of $\Gamma$ and the quantitative details of this diagram are not reliable at $\Gamma \sim J$. However, the topological structure of the diagram should be correct. This article is organized as follows. In Sec. II and III, the first and the second perturbation schemes will be presented (respectively) and we shall conclude with some discussions in Sec. IV.

## II. FIRST PERTURBATION SCHEME

### A. Principle

We shall now present a first-order perturbation calculation around $\kappa=0.5$ by rewriting the Hamiltonian $\mathcal{H}$ of Eq. (1) as

$$\mathcal{H} = \mathcal{H}_{cl} + \mathcal{H}_p,$$

where

$$\mathcal{H}_{cl} = -J \sum_j \left[ s_j^z s_{j+1}^z - \frac{1}{2} s_j^z s_{j+2}^z \right]. \tag{3}$$

and

$$\mathcal{H}_p = \sum_j \Gamma[-s_j^x + r s_j^z s_{j+2}^z], \tag{4}$$

with $r=J(\kappa-0.5)/\Gamma$. We always take $\Gamma$ to be positive, so that negative values of $r$ imply $\kappa < 0.5$.

We shall treat the $\mathcal{H}_p$ as a perturbation over $\mathcal{H}_{cl}$. Obviously, $\mathcal{H}_{cl}$ is the longitudinal (classical) part of $\mathcal{H}$ at $\kappa=0.5$ and $\mathcal{H}_p$ includes the transverse part and an increase of $\kappa$

(from 0.5) by an amount $r\Gamma$. One must note that for a perturbative treatment $\Gamma$ has to be small but $r$ need not be so. In the $(\kappa,\Gamma)$ phase space, the perturbation takes us from the multiphase point (0.5, 0) to a point $(0.5+r\Gamma/J,\Gamma)$. As $r$ varies from $-\infty$ to $\infty$, the perturbation takes us from the ferromagnetic to the antiphase region (Fig. 3). The first-order correction $(E^{(1)})$ to ground-state energy can be calculated *exactly*. This quantity is studied as a function of $r$, because if there is a nonanalyticity at $r=r_0$, then there will be a phase-transition line emanating from the (0.5,0) point at an angle $\tan^{-1}(1/r_0)$ with the increasing $\kappa$ direction. It is found that $E^{(1)}$ as a function of $r$ is nonanalytic only at $r=-0.5$ and 1. Therefore, only two lines of phase transition meet at the multiphase point. This implies either that the floating-paramagnetic transition line touches tangentially the floating-antiphase line at this point (Fig. 4) or that the floating phase extends over the entire region from the antiphase region to the ferromagnetic region (Fig. 2). It will be shown that a study of susceptibility and mass gap rules out the possibility of Fig. 4 and points to the validity of Fig. 2. Thus, the final conclusion from the first perturbation scheme is that the boundary between the ferromagnetic (antiphase) and the floating phase emanates from the multiphase point at an angle $\tan^{-1}-2(\tan^{-1}1)$ with the $\kappa$ axis. The second perturbation scheme also supports this conclusion and additionally
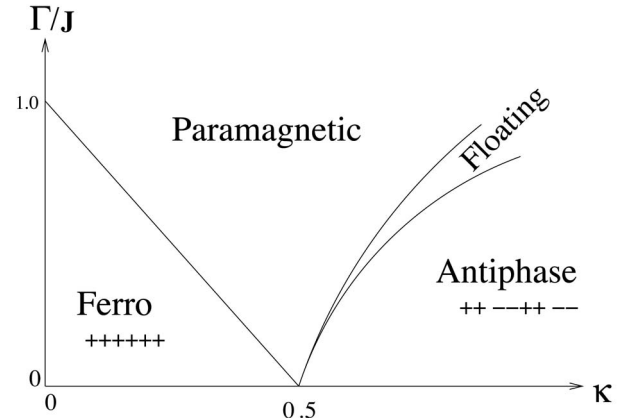


FIG. 4. One possible type of phase diagram of the transverse ANNNI model.

enables us to obtain an approximate phase diagram. We shall now transform our problem to a certain problem for the nearest-neighbor transverse Ising model and then through a study of the nearest-neighbor model, obtain the expression for $E^{(1)}$.

### B. Transformation to the nearest-neighbor model

We start by noting that at $\kappa = 0.5$ (the multiphase point [3]) the ground state of $\mathcal{H}_{cl}$, the unperturbed Hamiltonian, is a highly degenerate state and any spin configuration that has no spin domain of length unity (i.e., no $+ + - + +$- or $- - + - - $-type arrangement) can be the ground state. The number of domain walls is immaterial and can be anything between 0 and $N/2$, $N$ being the total number of spins. (Of course, for periodic boundary there can be only an even number of walls.) Let us denote the set of all such configurations as $\mathcal{S}$. Also, let the population of this set be $\nu$, which incidentally is of the order of $g^N$ as mentioned in Sec. I [3]. Now, the first-order correction to the eigenvalue are the eigenvalues of the $\nu \times \nu$ matrix $P$, whose elements are

$$P_{\alpha\beta} \equiv \langle \alpha | \mathcal{H}_p | \beta \rangle,$$

where $|\alpha\rangle$ and $|\beta\rangle$ are configurations within $\mathcal{S}$. The matrix $P$ can be easily given a block-diagonal structure. Note that $s_j^x |\beta\rangle \in \mathcal{S}$ if and only if the $j$th spin lies at the *boundary* of a domain, and the domain too has length larger than 2. Also, in such a case, $s_j^x$ operating on $|\beta\rangle$ will translate the wall at the left (right) of the $j$th site by one lattice spacing to the right (left). This immediately leads us to the important conclusion that $P_{\alpha\beta} \neq 0$ if and only if $|\alpha\rangle$ and $|\beta\rangle$ have an equal number of domain walls. Thus, we can break up $\mathcal{S}$ into subsets $\mathcal{S}(W)$, where $\mathcal{S}(W)$ contains all possible spin distributions with $W$ walls ($W = 2, 4, \ldots, N/2$). Now, the $\nu \times \nu$ matrix $P$ gets block diagonalized into matrices of size $\nu_W \times \nu_W$,

$$P_{\alpha\beta}(W) \equiv \langle \alpha | \mathcal{H}_p | \beta \rangle, \tag{5}$$

where $\nu_W$ is the population of $\mathcal{S}(W)$ and $|\alpha\rangle, |\beta\rangle \in \mathcal{S}(W)$. We now observe that the longitudinal term in $\mathcal{H}_p$ only contributes a diagonal term $r\Gamma(N-4W)$ to $P_{\alpha\beta}(W)$, so that one can write

$$P(W) = M(W) + r\Gamma(N - 4W)\mathbf{1}. \tag{6}$$

Here $\mathbf{1}$ is the $\nu_W \times \nu_W$ unit matrix, $M_{\alpha\beta}(W) \equiv \langle \alpha | \mathcal{H}_q | \beta \rangle$ and $\mathcal{H}_q = -\Gamma \sum_j s_j^x$ is the transverse part of $\mathcal{H}_p$. Thus the nontrivial problem is to solve the eigenproblem of $M(W)$.

To proceed with the matrices $M(W)$, let us construct from each member $|\alpha\rangle$ of $\mathcal{S}(W)$ a configuration $|\alpha'\rangle$ by removing one spin from each domain. The total number of spins in $|\alpha'\rangle$ will obviously be $N - W = N'$, say. Such a transformation was also used by Villain and Bak [9] for the case of the two-dimensional ANNNI model. The set $\mathcal{S}'(W)$ composed of the states $|\alpha'\rangle$ is then nothing but the set of all possible distributions of $N'$ spins with $W$ walls, with no restriction on the domains of length unity. It is easily seen that the matrix

$$M'_{\alpha\beta}(W) \equiv \langle \alpha' | \mathcal{H}_q | \beta' \rangle$$

will then be identical with $M(W)$ since the element

$$\left\langle \alpha' \left| \sum_{j=1}^{N'} s_j^x \right| \beta' \right\rangle$$

is nonzero when and only when

$$\left\langle \alpha \left| \sum_{j=1}^{N} s_j^x \right| \beta \right\rangle$$

is nonzero. The eigenproblem of $M'(W)$ becomes simple once we we observe that $S'(W)$ is nothing but the set of degenerate eigenstates of the Hamiltonian

$$\mathcal{H}'_0 = -J \sum_{j=1}^{N'} s_j^z s_{j+1}^z,$$

corresponding to the eigenvalue

$$E_W = -J(N' - 2W). \tag{7}$$

Thus, if we perturb $\mathcal{H}'_0$ by $\mathcal{H}_q$, then the first-order perturbation matrix will assume a block-diagonal form made up of the matrices $M'(W)$ for all possible values of $W$.

### C. Study of the nearest-neighbor model and further analysis

To solve the perturbation problem for $\mathcal{H}'_0 + \mathcal{H}_q$, we note that this Hamiltonian is the same as $\mathcal{H}$ of Eq. (1) with $\kappa = 0$, namely,

$$\mathcal{H}^{TI} = -\sum_{j=1}^{N'} [J s_j^z s_{j+1}^z + \Gamma s_j^x].$$

This is the Hamiltonian for the standard transverse Ising model. The exact solution for this Hamiltonian is readily available [2,13,14]. The exact expression for the energy eigenstates are (for periodic chain in the thermodynamic limit [15]),

$$E = 2\Gamma \sum_k \xi_k \Lambda_k, \tag{8}$$

where $\xi_k$ may be 0, $\pm 1$ and $k$ runs over $N'/2$ equispaced values in the interval 0 to $\pi$. Also, $\Lambda_k$ stands for $\sqrt{(\lambda^2 + 2\lambda \cos k + 1)}$, where $\lambda$ is the ratio $J/\Gamma$. For $\Gamma = 0$, the energy $E$ must be the same as $E_W$ of Eq. (7), so that

$$2 \sum_{k=0}^{\pi} \xi_k = -(N' - 2W). \tag{9}$$

Clearly, the different values of the quantity

$$\left( \frac{\partial E}{\partial \Gamma} \right)_{\Gamma=0} = 2 \sum_{k=0}^{\pi} \xi_k \cos k$$

correspond to the first-order perturbation corrections to the different levels. They are therefore also the eigenvalues of the $M'$ matrix. Thus the eigenvalues of the matrix $P(W)$ of Eq. (6) are

$$E_P = r\Gamma(N - 4W) + 2\Gamma\sum_{k=0}^{\pi} \xi_k \cos k. \qquad (10)$$

Keeping $N$ fixed we have to find, for which value of $W$ and for which distribution of $\xi_k$, $E_P$ is minimum subject to the constraint (9). For a given value of $\Sigma\xi_k$, this minimization is achieved if $-1$ values of $\xi_k$ accumulate near $k=0$ and $+1$ values near $k=\pi$. Let the desired distribution be

$$\xi_k = \begin{cases} -1 & \text{for } k = 0 \text{ to } \theta \\ 0 & \text{for } k = \theta \text{ to } \phi \\ 1 & \text{for } k = \phi \text{ to } \pi. \end{cases} \qquad (11)$$

Equation (9) now gives

$$N/N' = (4\pi - \theta - \phi)/2\pi, \qquad (12)$$

and one obtains

$$E_P = -\frac{N\Gamma}{4\pi - \theta - \phi}[r(4\pi - 3\theta - 3\phi) + 2(\sin\theta + \sin\phi)].$$

This quantity attains a minimum value only when $\theta$ and $\phi$ are equal and their common value ($\phi_0$, say) satisfies the condition

$$2\pi r = \sin\phi_0 + (2\pi - \phi_0)\cos\phi_0. \qquad (13)$$

The minimum value of $E_P$ is given by

$$E^{(1)} = -N\Gamma[3r - 2\cos\phi_0]. \qquad (14)$$

This is the exact expression for the first-order perturbation correction to ground-state energy. It is easily seen that for $r < -0.5$, that is, for $\Gamma/J < (1 - 2\kappa)$, one has $\phi_0 = \pi$ and $W = 0$ (ferromagnetic phase), while for $r > 1$, that is $\Gamma/J < (\kappa - 0.5)$, one has $\phi_0 = 0$ and $W = N/2$ (antiphase). As $r$ varies from $-1$ to $1$, $\phi_0$ gradually changes from $\pi$ to $0$ according to Eq. (13). The second derivative of $E^{(1)}$ with respect to $r$ blows up at $r = -0.5$ and $1$, indicating two critical lines there. One can see from Eq. (13) that except for these two values, $r$ is an analytic function of $\phi_0$ and hence, by Eq. (14), $E^{(1)}$ is also an analytic function of $r$. We have also checked explicitly (Appendix A) that no higher derivative of $E^{(1)}$ with respect to $r$ blows up at any other value of $r$.

As mentioned in Sec. II A, we can now conclude that the phase diagram is either like Fig. 2 or like Fig. 4.

### D. Study of longitudinal susceptibility

We shall now show that an analysis of longitudinal susceptibility points to the possibility of Fig. 2, rather than of Fig. 4. Let us call the eigenstate of $\mathcal{H}_0' + \mathcal{H}_q$ corresponding to $\theta = \phi = \phi_0$ as $|\psi'\rangle$. This state will be composed of the spin distributions that belong to $\mathcal{S}'(W)$ and can be written as

$$|\psi'\rangle = \sum_{j'} a_{j'}|j'\rangle,$$

where $|j'\rangle$ runs over all the states in $\mathcal{S}'(W)$. If we construct from each state $|j'\rangle$ another state $|j\rangle$ by adding one spin to each domain, and then combine these states with the same coefficients, then we arrive at a state $\Sigma_j a_j|j\rangle$, where $a_j = a_{j'}$.

This is an eigenstate of $M(W)$ and hence of $P(W)$ [see Eq. (6)] and this eigenstate is nothing but the zeroth-order eigenfunction $|\psi^{(0)}\rangle$ for the perturbed ground state of $\mathcal{H}_{cl} + \mathcal{H}_p$. One should observe that although the spin-spin correlation may not be equal for $|j\rangle$ and $|j'\rangle$, the longitudinal magnetization $M_z$ must be the same for them (an equal number of positive and negative spins are added while transforming $|j'\rangle$ to $|j\rangle$). Thus, the longitudinal susceptibility

$$\chi_z \propto \langle M_z^2\rangle - \langle M_z\rangle^2$$

of $|\psi^{(0)}\rangle$ must be the same as that of $|\psi'\rangle$. The spin-spin correlation

$$C^z(n) \equiv \langle s_i^z s_{i+n}^z\rangle$$

for $|\psi'\rangle$ may be calculated (see Appendix B). In the case of $\Gamma < J$, for the entire range $0 < \phi_0 < \pi$, the correlation is

$$C^z(n) = A\frac{1}{\sqrt{n}}\cos[n(\pi - \phi_0)],$$

where $A$ is a constant. This is clearly a floating phase. The susceptibility $\chi_z$ is hence infinity for both the states $|\psi'\rangle$ and $|\psi^{(0)}\rangle$. This leads us to the conclusion that the zeroth-order eigenstate is in floating phase and hence, at least for small values of $\Gamma$, the ground state of the transverse ANNNI chain must be a floating phase for all values of $r$ between $-0.5$ and $1$. Of course, for large values of $\Gamma$ the perturbation corrections may cancel the divergence of susceptibility and lead to a paramagnetic state.

One must note that it is difficult to derive an *exact* relationship between the correlation in state $|\psi^{(0)}\rangle$ and the same in state $|\psi'\rangle$. Although a similar relationship was obtained by Villain and Bak [9], we do not extend that derivation here. It is interesting to note that Villain and Bak (and also Uimin and Rieger [4]) assumed the wave number to be equal to half the number of domain walls per site, but we shall soon find that this conclusion disagrees with the results obtained from our second perturbation scheme.

### E. Study of mass gap

We shall now show that an analysis of mass gap also points to the possibility of Fig. 2, rather than of Fig. 4, thus agreeing with the conclusion from the analysis of longitudinal susceptibility. One signature of floating phase or diverging correlation length is vanishing *mass gap* [2,16]. Let us now study the first-order (in $\Gamma$) correction to the mass gap. Since the first-order correction to all energy states is given by the different possible values of $E_P$ of Eq. (10), the correction to the energy of the first excited state is the smallest possible value of $E_P$ apart from the ground state $E^{(1)}$. To find the lowest excitation over the ground state, we note that such excitation is possible either (i) by keeping $\Sigma\xi_k$ fixed and rearranging the $\xi_k$ values; or (ii) by altering $\theta$ and $\phi$ and thus altering $\Sigma\xi_k$. For (i) the lowest excitation will correspond to an interchange of $+1$ and $-1$ at $k = \phi_0$, which will lead to a mass gap (for the whole system, not per site)

$$\Delta^{(1)} = \frac{8\pi\Gamma\lambda\sin\phi_0}{N'\Lambda_{\phi_0}}.$$

For (ii) the mass gap is

$$\Delta^{(1)} = \frac{1}{2}\left(\frac{\partial^2 E_P}{\partial\theta^2}\right)_{\theta=\phi_0}(\delta\theta)^2.$$

Here $\delta\theta$ is the smallest possible deviation in $\theta$ at $\phi_0$. As the smallest possible change in $W$, and hence in $N'$ is 2, Eq. (12) (with $\theta=\phi$) tells us that

$$\delta\theta = \frac{2(2\pi-\theta)^2}{\pi N} \sim \frac{1}{N}.$$

This shows that for both the mechanisms (i) and (ii), the mass gap $\Delta^{(1)}$ vanishes as $N\to\infty$ for all values of $\phi_0$ between 0 and $\pi$. This shows that for all values of $r$ between $-0.5$ and 1 there must be a floating phase for small $\Gamma$.

For transverse Ising model ($\kappa=0$) the phase transition occurs at $\Gamma=J$ and at $\Gamma=J+\epsilon$ the first-order correction to the mass gap is just $\epsilon$, and is thus nonvanishing, indicating that the divergent correlation length does not extend beyond $\Gamma=J$.

## III. SECOND PERTURBATION SCHEME

### A. Principle

In the previous section we have found that the phase diagram looks like Fig. 2. In order to confirm this result explicitly, we have to know the eigenfunction with first- or even zeroth-order correction. As it is difficult to calculate the eigenfunction for the perturbation scheme discussed above in Sec. II, we shall perform the second set of perturbation calculation now.

Let us write the Hamiltonian $\mathcal{H}$ of Eq. (1) for $\kappa<0.5$ as

$$\mathcal{H} = N(h_0 + h_1 - J\kappa), \qquad (15)$$

with

$$h_0 = -(1-2\kappa)J\frac{1}{N}\sum_j s_j^z s_{j+1}^z - \Gamma\frac{1}{N}\sum_j s_j^x \qquad (16)$$

and

$$h_1 = \kappa J\frac{1}{N}\sum_j (1 - s_j^z s_{j+1}^z)(1 - s_{j+1}^z s_{j+2}^z). \qquad (17)$$

Clearly, $h_0$ represents the Hamiltonian of the standard transverse Ising model with nearest-neighbor interaction and $h_1$ represents the number of domains of length 1. We shall treat the operator $h_1$ as the perturbation on the Hamiltonian $h_0$. All the eigenstates of $h_0$ are precisely known [14] and for each eigenstate one can readily calculate the expectation value of $h_0+h_1$ and identify the eigenstate for which $\langle h_0+h_1\rangle$ is the lowest. This state is the eigenstate with zeroth-order perturbation correction. Therefore, the basic idea is to identify the ground state up to first-order perturbation correction to eigenvalue. We carry on this scheme for all values of $\kappa(<0.5)$ and $\Gamma$ and in each case calculate the correlation
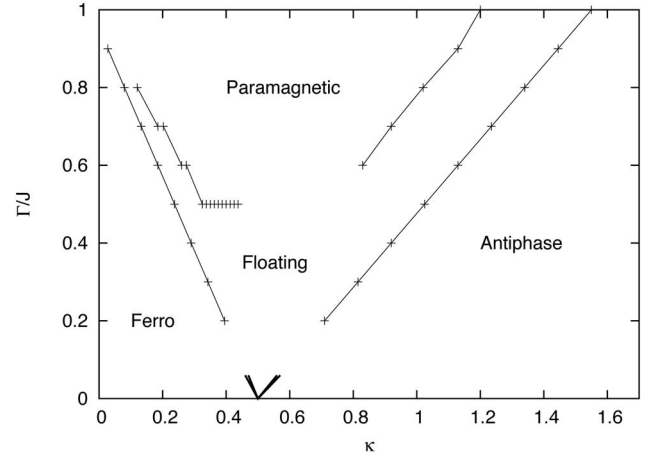


FIG. 5. Phase diagram of the transverse ANNNI model as obtained from the first and the second-perturbation scheme. The thick lines are exact results from the first perturbation scheme. The thin lines are approximate results from the second perturbation scheme. The thin line is not drawn in the region where the latter scheme becomes unreliable.

function [as defined in Eq. (2)] and characterize the phase therefrom.

Indeed, our results are reliable only for small values of $\langle h_1\rangle$. Hence, this quantity must be small for the low-lying eigenstates of $h_0$. As mentioned already, the operator $h_1$ basically counts the number of domains of length 1. For $\kappa<0.5$ the ground state of $h_0$ at $\Gamma=0$ is ferromagnetic and the low-energy states may be expected to have small $\langle h_1\rangle$ and the perturbation treatment will be justified for small values of $\Gamma$. However, for $\kappa>0.5$, the ground state of $h_0$ will be antiferromagnetic (having domains of length 1 only) and such a perturbation scheme is not valid.

For $\kappa>0.5$ one can break up $\mathcal{H}$ as

$$\mathcal{H} = N(h_0' + h_1' - 0.5J), \qquad (18)$$

with the unperturbed Hamiltonian defined as

$$h_0' = (\kappa-0.5)J\frac{1}{N}\sum_j s_j^z s_{j+2}^z - \Gamma\frac{1}{N}\sum_j s_j^x, \qquad (19)$$

and the perturbation as

$$h_1' = 0.5J\frac{1}{N}\sum_j (1 - s_j^x s_{j+1}^z)(1 - s_{j+1}^z s_{j+2}^z). \qquad (20)$$

The Hamiltonian $h_0'$ represents a chain with only next-nearest-neighbor interaction and the operator $h_0'$ counts (as for $\kappa<0.5$) the number of domains of length 1. The ground state of $h_0'$ at $\Gamma=0$ is antiphase, and hence has $\langle h_1'\rangle=0$, so that the perturbation scheme is justified. Following the principle for the previous case, one can identify numerically the eigenstate (of $h_0'$) for which $\langle h_0'+h_1'\rangle$ is a minimum. From the correlation function of this state, one can characterize the phase.

The phase diagram obtained from the analysis of the present section is shown in Fig. 5. It has the following fea-
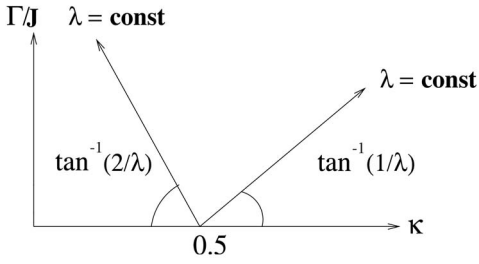
FIG. 6. Plot of $\lambda = $ constant line.

tures: (i) The floating phase exists and extends from the ferromagnetic phase to the antiphase for small $\Gamma$; thus Fig. 2 rather than Fig. 4 is the type of the phase diagram. (ii) There is a line along which transition from floating phase to paramagnetic phase takes place; this line for $\kappa < 0.5$ [obtained using Eq. (15)] continues smoothly to the same for $\kappa > 0.5$ [obtained using Eq. (18)].

We shall now present the details of the calculation for the two ranges of $\kappa$.

### B. For $\kappa < 0.5$

The Hamiltonian $h_0$ of Eq. (16) corresponds to the nearest-neighbor transverse Ising model with (ferromagnetic) interaction strength $(1 - 2\kappa)J$. Following Eq. (8), the eigenstates of this operator are

$$\langle h_0 \rangle = \Gamma \frac{1}{N/2} \sum_k \xi_k \Lambda_k, \qquad (21)$$

with $\Lambda_k = \sqrt{(\lambda^2 + 2\lambda \cos k + 1)}$ as in Sec. II, but $\lambda = (1 - 2\kappa)J/\Gamma$. The line corresponding to a constant value of $\lambda$ is now a straight line at an angle $\tan^{-1}(2/\lambda)$ with the $\kappa$ axis (Fig. 6). For each eigenstate, the $n$th-neighbor longitudinal correlation function [defined by Eq. (2)] can be expressed as the Toeplitz determinant [14]

$$C^z(n) = \begin{vmatrix} G_0 & G_{-1} & G_{-2} & \cdots & G_{-n+1} \\ G_1 & G_0 & G_{-1} & \cdots & G_{-n+2} \\ G_2 & G_1 & G_0 & \cdots & G_{-n+3} \\ \cdots \\ G_{n-1} & G_{n-2} & G_{n-3} & \cdots & G_0 \end{vmatrix}, \qquad (22)$$

where the elements are given by

$$G_j = -\frac{2}{N} \sum_{k=0}^{\pi} \frac{\xi_k}{\Lambda_k} [\cos(kj - k) + \lambda \cos(kj)]. \qquad (23)$$

Here, the wave vector $k$ runs over the $N/2$ equispaced values in the interval 0 to $\pi$ and $\xi_k$ can be 0 or $\pm1$ for each of the $N/2$ values of $k$ between 0 and $\pi$.)

Now, for any eigenstate of $h_0$, the expectation value of $h_1$ can be calculated first by rewriting it as

$$h_1 = \kappa J \frac{1}{N} \sum_j (1 - 2s_j^z s_{j+1}^z + s_j^z s_{j+2}^z),$$

and then evaluating the first- and second-neighbor correlation functions using Eq. (22). The result is

$$\langle h_1 \rangle = \kappa J[(1 - G_0)^2 - G_1 G_{-1}]. \qquad (24)$$

To find which distribution of $\xi_k$ gives the smallest value of $\langle h_0 + h_1 \rangle$, we note that $G_0$ will be closest to 1, when the $(-1)$ values of $\xi_k$ accumulate near $k = 0$ and $(+1)$ values near $k = \pi$. Although Eq. (24) does not clearly indicate that such a distribution of $\xi_k$ will also lead to the largest values of $G_1$ and $G_{-1}$, we have verified by going through *all* the $2^N$ states (for $N = 12$) that indeed such a distribution leads to the lowest value of $\langle h_0 + h_1 \rangle$. We can now assume the distribution of $\xi_k$ values to be the same as described in Eq. (11) and calculate $\langle h_0 + h_1 \rangle$ for given values of $\theta$ and $\phi$. For every $\kappa$ and $\Gamma$, we take a system of 1000 spins and consider all possible choices of $\theta$, $\phi$ and note the values (say, $\theta_0$ and $\phi_0$) for which $\langle h_0 + h_1 \rangle$ attains a minimum. For the entire parameter range investigated in this work, we found $\theta_0 = \phi_0$. Equation (11) now reduces to (with $\theta = \phi = \phi_0$) a distribution, namely,

$$\xi_k = \begin{cases} -1 & \text{for } k = 0 \text{ to } \phi_0 \\ 1 & \text{for } k = \phi_0 \text{ to } \pi. \end{cases} \qquad (25)$$

This corresponds to our approximate ground-state eigenfunction for $\mathcal{H}$. We have also found that for this eigenfunction, $\langle h_1 \rangle$ is nonzero. As $\langle h_1 \rangle$ is zero for all the ground-state eigenfunctions at $\Gamma = 0$, we may conclude that the state we have determined as the ground state of $h_0 + h_1$, is an excited state of $h_0$. In this connection, we point out that for the 2D ANNNI model, it has been proved that [17] if one neglects completely the domains of length 1 (i.e., assumes $\langle h_1 \rangle$ to be zero), then one misses the floating phase, indicating that the floating phase consists of states that do *not* belong to the ground state at the $(T, \kappa) = (0, 0.5)$ point.

For every value of $\kappa$ and $\Gamma$ we now have determined the value of $\phi_0$ and Eq. (25) therefore gives us the ground-state eigenfunction. This leads to an expression for the correlation function $C^z(n)$ of Eq. (22) in the form of a determinant, an analytic expression of which has been given in Appendix B for large values of $n$. The final result is as follows. For $\lambda > 1$, that is, $\Gamma/J < (1 - 2\kappa)$, the value of $\phi_0$ turns out to be $\pi$, leading to a ferromagnetic phase. For $\lambda < 1$, that is, $\Gamma/J > (1 - 2\kappa)$, there are two regions. In one region $\phi_0 < \pi$ and according to Appendix B, the correlation is

$$C^z(n) = A(\phi_0) \frac{1}{\sqrt{n}},$$

indicating a floating phase with index 0.5 and no modulation. The parameter $\phi_0$ varies continuously as a function of $\kappa$ and $\Gamma$ (Fig. 7), but this variation affects only the amplitude $A$. In the other region, $\phi_0 = \pi$, and the correlation is exponentially decaying, indicating a paramagnetic phase. The values of $\lambda$ and $\phi_0$ and the corresponding phases in different portions of the phase diagram are indicated in Fig. 8. The phase diagram thus obtained agrees with the conclusions from our first perturbation scheme and is presented in Fig. 5.

### C. For $\kappa > 0.5$

The Hamiltonian $h_0'$ of Eq. (18) corresponds to a chain ($\mathcal{C}$, say) with only next-nearest-neighbor interaction and can be
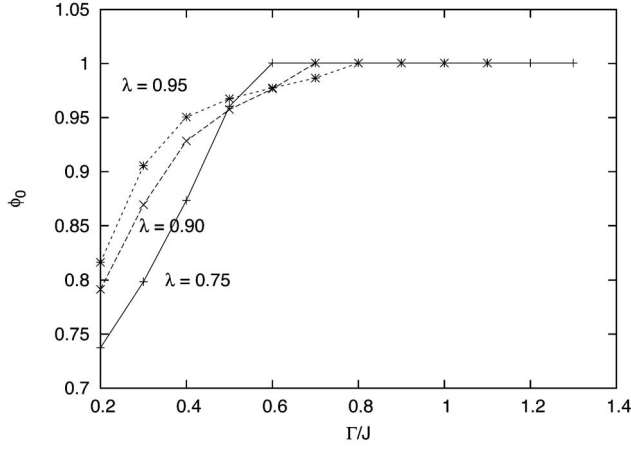
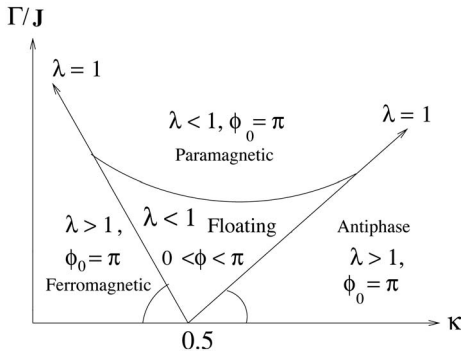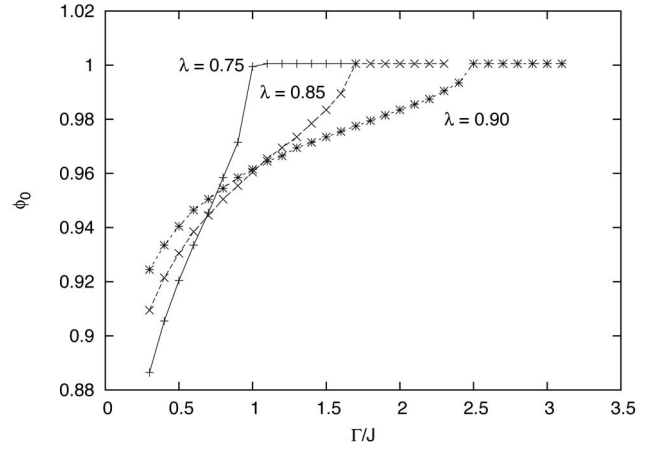FIG. 7. Plot of $\phi_0$ (unit$=\pi$) vs $\Gamma$ for $\kappa < 0.5$.

broken into two independent transverse Ising chains ($\mathcal{C}_1$ and $\mathcal{C}_2$, say) each having nearest-neighbor antiferromagnetic interaction. Hence, the correlation $\Sigma s_j^z s_{j+1}^z$ in $\mathcal{C}$ will be zero and $\Sigma_j s_j^z s_{j+2}^z$ in $\mathcal{C}$ will be the same as the nearest-neighbor correlation in the constituent chains $\mathcal{C}_1$ and $\mathcal{C}_2$. (Indeed, $\mathcal{C}_1$ and $\mathcal{C}_2$ will be uncorrelated because, any configuration of $\mathcal{C}_1$ will couple with equal probability to two configurations of $\mathcal{C}_2$, one of which can be obtained from the other by reversing all spins.) Moreover, since each of the antiferromagnetic chains can be transformed to a ferromagnetic chain ($\mathcal{C}_0$, say) by simply reversing the alternate spins, the eigenstates of $h_0'$ in $\mathcal{C}$ are related to the eigenstates of a nearest-neighbor ferromagnetic transverse Ising chain $\mathcal{C}_0$. We have then,

$$\langle h_0' \rangle = \Gamma \frac{1}{N/2} \sum_k \xi_k \Lambda_k \qquad (26)$$

and

$$\langle h_1' \rangle = 0.5J(1 - G_0), \qquad (27)$$

with $G_0$ defined by Eq. (23) but now with $\lambda = (\kappa - 0.5)J/\Gamma$. As before, $k$ runs over $N/2$ equispaced values in the interval 0 to $\pi$. The $\lambda=$ constant line is now a straight line at an angle $\tan^{-1}(1/\lambda)$ with the $\kappa$ axis (Fig. 6). As in the previous subsection, we look for the eigenstate (i.e., the $\xi_k$ distribution) for which $\langle h_0' + h_1' \rangle$ will be lowest and observe that $G_0$ will be



FIG. 8. Schematic phase diagram showing the values of $\lambda$ and $\phi_0$ in different portions.

largest when the $(-1)$ values of $\xi_k$ accumulate near $k=0$ and $(+1)$ values near $k=\pi$. Also, investigating all the states for a chain of only 12 spins, we find that the minimum value of $\langle h_0' + h_1' \rangle$ corresponds to the distribution with no zero values of $\xi_k$. Thus, assuming the distribution of Eq. (25), we can find numerically the value of $\theta$ (say, $\phi_0$) for which $\langle h_0' + h_1' \rangle$ will be lowest for a chain of 1000 spins. It is found that this minimum corresponds to a nonzero value of $\langle h_1' \rangle$, indicating that as for $\kappa < 0.5$, the unperturbed state corresponding to the ground state is an excited state of $h_0'$.

As in the previous subsection, we can use the expression for $C^z(n)$ mentioned in Appendix B as the correlation in the chain $\mathcal{C}_0$. The corresponding spin-spin correlation in the ANNNI chain $\mathcal{C}$ will be

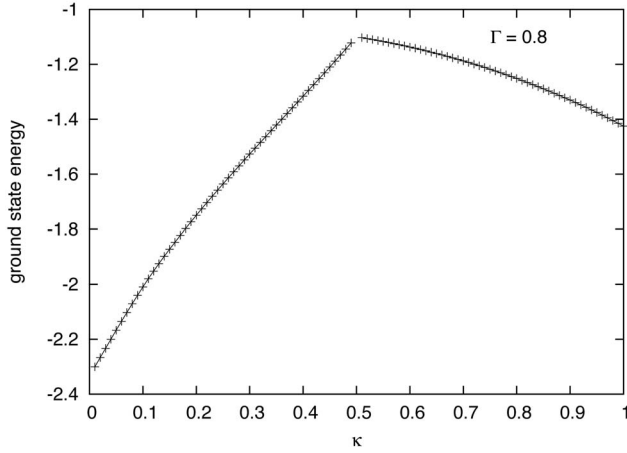$$C_A^z(n) = \begin{cases} 0 & \text{for odd } n \\ (-1)^n C^z(n/2) & \text{for even } n. \end{cases}$$

In this expression, the $(-1)^n$ factor takes account of the mapping between the ferromagnetic and antiferromagnetic chains. The final result is as follows. For $\lambda > 1$, that is, $\Gamma/J < (\kappa - 0.5)$, the value of $\phi_0$ turns out to be $\pi$, so that the correlation in the chain $\mathcal{C}_0$ is constant and the correlation $C_A^z(n)$ corresponds to a perfect antiphase. For $\lambda < 1$, that is, $\Gamma/J > (\kappa - 0.5)$, there are two regions. In one region $\phi_0 < \pi$ and according to Appendix B, the correlation is

$$C_A^z(n) = A(\phi_0) \cos\left(\frac{n\pi}{2}\right) \frac{1}{\sqrt{n}}, \qquad (28)$$

indicating a floating phase with index 0.5 and modulation

$$q = \pi/2.$$

The parameter $\phi_0$ varies continuously as a function of $\kappa$ and $\Gamma$ (Fig. 9), but this variation affects only the amplitude $A$. In the other region, $\phi_0 = \pi$, and the correlation in $\mathcal{C}_0$ is exponentially decaying, indicating a paramagnetic phase with the



FIG. 9. Plot of $\phi_0$ (unit$=\pi$) vs $\Gamma$ for $\kappa > 0.5$.

FIG. 10. Plot of ground-state energy vs $\kappa$ for $\Gamma/J = 0.8$.



FIG. 11. Plot of the nearest-neighbor correlation as a function of $\Gamma$ (in unit of $J$) for $\lambda = 0.75$, 0.90, and 0.95.

same modulation. The values of $\lambda$ and $\phi_0$ and the corresponding phases in different portions of the phase diagram is indicated in Fig. 8 and the resulting phase diagram is presented in Fig. 5, which agrees with the conclusions from our first perturbation scheme.

## IV. DISCUSSION

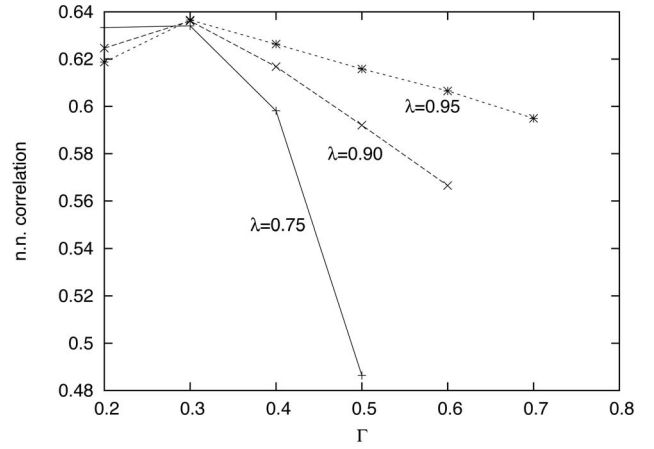In this section we shall point out some features of the phase diagram we have obtained.

(1) In the floating phase ($\lambda < 1$) the spin-spin correlation decays as

$$C^z(n) = A \frac{1}{n^\eta},$$

with $\eta = 0.5$. It is interesting to note that on the boundary between the floating and the ordered (ferromagnetic or antiphase) state $\lambda$ is 1 and $\phi_0$ is 0 or $\pi$ and the correlation decays algebraically with $\eta = 0.25$ as shown by Pfeuty [14]. Thus, the value of the index undergoes a nonanalytic change at the boundary.

(2) In the floating phase, the correlation is nonoscillatory ($q=0$) for $\kappa < 0.5$ and oscillatory ($q=\pi/2$) for $\kappa > 0.5$. Hence, the line $\kappa = 0.5$ is the "disorder line" [3] across which the modulation wave vector suffers a sudden change from 0 to $\pi/2$. We have also measured the perturbed energy $\langle h_0 \rangle + \langle h_1 \rangle$ and $\langle h_0' \rangle + \langle h_1' \rangle$ on two sides of the disorder line for a given $\Gamma$ (Fig. 10). This energy remains continuous but suffers a change of slope at $\kappa = 0.5$. Since the first perturbation scheme does not indicate any phase transition around $\kappa = 0.5$, we guess that this change of slope is not the signature of any serious nonanalytic behavior but is only an outcome of the approximation inherent in perturbation calculation.

(3) Within the floating phase, for $\kappa > 0.5$, the nearest-neighbor correlation is zero [Eq. (28)] and the wave vector is $q = \pi/2$, implying that the wave number $q/2\pi$ is equal to half the number of domain walls per site. On the other hand, for $\kappa < 0.5$, the nearest-neighbor correlation is not at all zero (Fig. 11), but the correlation is nonoscillatory ($q=0$), imply-

ing that the wave number $q/2\pi$ is *not* equal to half the number of domain walls per site. One must note that (as mentioned above), the analytic treatments of Villain and Bak [9], and of Uimin and Rieger [4] assumes the equality of the wave number and half the number of domain walls per site. This assumption thus agrees with our results for $\kappa > 0.5$ but not for $\kappa < 0.5$.

(4) The second perturbative scheme would be reliable only when the ratio $\langle h_1 \rangle / \langle h_0 \rangle$ or $\langle h_1' \rangle / \langle h_0' \rangle$ (accordingly as $\kappa$ is $<0.5$ or $>0.5$) is small. We have included in Fig. 5 only those points where this ratio is less than some arbitrarily chosen number $1/3$. This criterion made us unable to locate the boundary between the paramagnetic and floating phase near $\kappa = 0.5$, $\Gamma = 0$ resulting in a gap there in Fig. 5. Some better approximation is needed to bridge this gap.

(5) The first and second perturbation schemes can be compared and reconciled in the following way. For the first perturbation scheme, the unperturbed Hamiltonian corresponds to the $\kappa = 0.5$, $\Gamma = 0$ point, and the exact expressions for the first-order correction to energy gives exactly the directions along which the boundaries of ferromagnetic phase and antiphase emanate from this point (see Fig. 5). On the other hand, for the second perturbation scheme, the unperturbed Hamiltonian corresponds to the boundary lines of the ferromagnetic phase and the antiphase since on these lines $\langle h_1 \rangle$ and $\langle h_1' \rangle$ are zero. The approximate estimate of the first-order correction to energy gives the nature of the phase near the boundary. However, since the estimate is only approximate, at some regions of the parameter space, it is not reliable (as explained above).

(6) It has been shown [7] that along the *Peschel-Emery line* $\Gamma/J = 1/(4\kappa) - \kappa$, the ground state for the transverse ANNNI Hamiltonian $\mathcal{H}$ can be solved exactly. This line turns out to be the disorder line and along it, the correlation length is very small. This line touches tangentially our ferromagnetic boundary at $\Gamma = 0$, but deviates from our approximate disorder line ($\kappa = 0.5$) at $\Gamma > 0$. Note that our treatment is unreliable in the $\kappa \approx 0.5$ region anyway.

## APPENDIX A: HIGHER DERIVATIVES FOR THE FIRST-ORDER PERTURBATION CORRECTION

We have derived earlier an expression

$$E^{(1)} = -N\Gamma \frac{2\sin\phi_0 + 2\pi r - 3r\phi_0}{2\pi - \phi_0}$$

for the first-order correction to the ground-state energy of the Hamiltonian [see Eq. (3)]

$$\mathcal{H}_{cl} = -J\sum_j \left[ s_j^z s_{j+1}^z - \frac{1}{2} s_j^z s_{j+2}^z \right]$$

under perturbation by the Hamiltonian [see Eq. (4)]

$$\mathcal{H}_p = \sum_j \Gamma[-s_j^x + r s_j^z s_{j+2}^z].$$

In this Appendix we shall show by the method of induction, that for all values of $\phi_0$ in the range $0 < \phi_0 < \pi$, all higher derivatives of this quantity $E^{(1)}$ remain finite. For this purpose, we note that the first- and second-order derivatives are

$$\frac{\partial E^{(1)}}{\partial r} = -N\Gamma \left( -\frac{4\pi}{(2\pi - \phi_0)} + 3 \right)$$

and

$$\frac{\partial^2 E^{(1)}}{\partial r^2} = -N\Gamma \left( \frac{8\pi^2}{(2\pi - \phi_0)^3 \sin\phi_0} \right).$$

Here we have used the equality

$$\frac{\partial \phi_0}{\partial r} = \frac{2\pi}{(2\pi - \phi_0)\sin\phi_0},$$

which can be obtained from Eq. (13). Thus, at least for $m = 1$ and 2 the derivatives can be expressed in the form

$$\frac{\partial^m E^{(1)}}{\partial r^m} = -N\Gamma \sum_{i=1}^{m'} k_i \frac{\cos^{\alpha_i}\phi_0}{(2\pi - \phi_0)^{\beta_i}\sin^{\gamma_i}\phi_0}, \qquad \text{(A1)}$$

where $m' \sim 3^m$, and $\alpha_i, \beta_i, \gamma_i, k_i$ are constants $\geq 0$ with the restriction $\gamma_i \leq \alpha_i$ (except for $m = 1$, where $\alpha_i = \gamma_i = 0$). Differentiating Eq. (A1) once, it can be easily verified that the form (A1) should be valid for $m + 1$ also, and is hence valid for all values of $m$. Since the right-hand side of Eq. (A1) diverges only when $\sin\phi_0$ vanishes, we conclude that so long as $\phi_0$ is neither 0 or $\pi$ the higher derivatives of $E^{(1)}$ remain finite.

## APPENDIX B: LONG-RANGE CORRELATION FOR THE EXCITED STATES

Here we shall consider the transverse Ising model with the nearest-neighbor interaction described by the Hamiltonian

$$\mathcal{H}^{TI} = -\sum_{j=1}^{N} [J s_j^z s_{j+1}^z + \Gamma s_j^x]. \qquad \text{(B1)}$$

The exact solution [2,13,14] for this Hamiltonian tells us that the $2^N$ number of energy eigenvalues are

$$E = 2\Gamma \sum_k \xi_k \Lambda_k, \qquad \text{(B2)}$$

where $\Lambda_k = \sqrt{(\lambda^2 + 2\lambda\cos k + 1)}$, $\lambda = J/\Gamma$, $\xi_k$ may be 0, $\pm 1$ and $k$ runs over $N/2$ equispaced values in the interval 0 to $\pi$.

In the text we have come across (more than once) the $\xi_k$ distribution of the following type:

$$\xi_k = \begin{cases} -1 & \text{for } k = 0 \text{ to } \phi \text{ (unexcited)} \\ 1 & \text{for } k = \phi \text{ to } \pi \text{ (excited)}. \end{cases} \qquad \text{(B3)}$$

This is an excited state and reduces to the ground state only for $\phi = \pi$. This state is important for this work because it corresponds to the ground state after perturbation in the second perturbation scheme [Eq. (25)]. It also corresponds to the first-order correction in the first perturbation scheme [Eq. (11)]. We shall present in this Appendix the expressions for the longitudinal two-spin correlation function

$$C^z(n) \equiv \langle s_j^z s_{j+n}^z \rangle - \langle s_j^z \rangle^2 \qquad \text{(B4)}$$

(for $n \ll N$) in the long-range limit $n \to \infty$.

Let us consider the quantity

$$\sigma^z(n) \equiv \langle s_j^z s_{j+n}^z \rangle \qquad \text{(B5)}$$

remembering that,

$$\lim_{n \to \infty} \sigma^z(n) = \langle s_j^z \rangle^2.$$

Standard treatise [2,13,14] show that for $\phi = \pi$ (no excited state), this quantity is of the following form. For $\lambda > 1$,

$$\sigma^z(n) = \left( 1 - \frac{1}{\lambda^2} \right)^{1/4} + A\exp(-\alpha n)$$

($A, \alpha$ are constants depending on $\lambda$). This corresponds to the ferromagnetic state. For $\lambda < 1$,

$$\sigma^z(n) = A'\exp(-\alpha' n)$$

($A', \alpha'$ are constants depending on $\lambda$). This corresponds to the paramagnetic state. There is a nonanalyticity at the point $\lambda = 1$, where the second derivative of ground-state energy diverges.

Let us consider the correlation function $C^z(n)$ when $\lambda \neq 1$ and $0 < \phi < \pi$ (i.e., $\phi \neq 0$ and $\phi \neq \pi$—some, but not all states are excited). We shall show elsewhere [18] that this quantity can be calculated exactly using Szego's theorem. The results obtained are as follows. The quantity

$\lim_{n \to \infty} \sigma^z(n)$ will be zero, so that $C^z(n)$ and $\sigma^z(n)$ are equal. Also, for $\lambda > 1$,

$$C^z(n) = \frac{0.590}{\sqrt{\sin \phi}}\left(1 - \frac{1}{\lambda^2}\right)^{1/4}\frac{\cos(\pi + \phi)n}{\sqrt{n}}, \qquad \text{(B6)}$$

and for $\lambda < 1$,

$$C^z(n) = \frac{0.590\sqrt{\sin \phi}}{\sqrt{(1 + \lambda^2 + 2\lambda \cos \phi)}}(1 - \lambda^2)^{1/4}\frac{1}{\sqrt{n}}. \qquad \text{(B7)}$$

These expressions have been used in the text (Secs. II D, III B, and III C) for the analysis of the phase diagram of the 1D transverse ANNNI model.

[1] B. K. Chakrabarti, A. Dutta, and P. Sen, *Quantum Ising Phases and Transitions in Transverse Ising Models* (Springer-Verlag, Berlin, Heidelberg, 1996).

[2] D. C. Mattis, *The Theory of Magnetism*, (Springer-Verlag, Berlin, Heidelberg, 1985), Vol. II, Sec. 3.6.

[3] W. Selke, Phys. Rep. **170**, 213 (1988).

[4] G. Uimin and H. Rieger, Z. Phys. B: Condens. Matter **101**, 597 (1996).

[5] C. M. Arizmendi, A. H. Rizzo, L. N. Epele, and C. A. Garcia, Z. Phys. B: Condens. Matter **83**, 273 (1991).

[6] P. Sen, S. Chakrabarty, S. Dasgupta, and B. K. Chakrabarti, Z. Phys. B: Condens. Matter **88**, 333 (1992).

[7] A. Dutta and D. Sen, Phys. Rev. B **67**, 094435 (2003).

[8] W. Selke and M. E. Fisher, Z. Phys. B: Condens. Matter **40**, 71 (1980); W. Selke, *ibid.* **43**, 335 (1981).

[9] J. Villain and P. Bak, J. Phys. (Paris) **42**, 657 (1981).

[10] T. Shirahata and T. Nakamura, Phys. Rev. B **65**, 024402 (2001).

[11] R. Derian, A. Gendiar, and T. Nishino, e-print cond-mat/0605411.

[12] A. K. Chandra and S. Dasgupta (unpublished).

[13] E. Lieb, T. Schultz, and D. C. Mattis, Ann. Phys. (N.Y.) **16**, 407 (1961).

[14] P. Pfeuty, Ann. Phys. (N.Y.) **57**, 79 (1970).

[15] The boundary condition for the exact solution is discussed in Mattis [2], Sec. 3.7.

[16] S. Sachdev, *Quantum Phase Transitions* (Cambridge University Press, Cambridge, England, 1999), Chaps. 1 and 3.

[17] S. Dasgupta, Phys. Lett. A **146**, 181 (1990).

[18] A. K. Chandra and S. Dasgupta (unpublished).